

Classification of pepper seeds using machine vision based on neural network

Ferhat Kurtulmuş^{1*}, İlknur Alibas¹, Ismail Kavdir²

(1. Department of Biosystems Engineering, Faculty of Agriculture, Uludag University, 16059 Bursa, Turkey;

2. Department of Agricultural Machinery, Faculty of Agriculture, Canakkale Onsekiz Mart University, 17100 Canakkale, Turkey)

Abstract: Pepper is widely planted and used all over the world as fresh vegetable and spice. Genetic and morphological information of pepper are stored through seeds. Determination of seed variety is crucial for correctly identifying genetic materials. Pepper varieties cannot be easily classified even by an expert eye due to the very small size of seeds and visual similarities. Hence, more advanced technologies are required to determine the variety of a pepper seed. A classification method was proposed to discriminate pepper seed based on neural networks and computer vision. Image acquisition was conducted using an office scanner at a resolution of 1200 dpi. Image features representing color, shape, and texture were extracted and used to classify pepper seeds. By calculating features from different color components, a feature database was constructed. Effective features were selected using sequential feature selection with different criterion functions. As a result of the feature selection procedure, the number of the features was significantly reduced from 257 to 10. Cross validation rules were applied to obtain a reliable classification model by preventing overfitting. Different numbers of neurons in the hidden layer and various training algorithms were investigated to determine the best multilayer perceptron model. The best classification performance was obtained using 30 neurons in the hidden layer of the network. With this network, an accuracy rate of 84.94% was achieved using the sequential feature selection and the training algorithm of resilient back propagation in classifying eight pepper seed varieties.

Keywords: pepper seed, neural networks, variety classification, computer vision

DOI: 10.3965/j.ijabe.20160901.1790

Citation: Kurtulmuş F, Alibas İ, Kavdir I. Classification of pepper seeds using machine vision based on neural network. Int J Agric & Biol Eng, 2016; 9(1): 51–62.

1 Introduction

Identification of variety is crucial in agricultural industry. For ensuring the correct product is planted and harvested, growers want to know the variety of the seed

they plant especially at purchase stage of the seed. Correct discrimination of seed in specific agricultural markets enables bulk buyers to ensure that only desired variety is supplied^[1]. Moreover, foreign pollination during seed growing may occur so that undesired seeds or varieties take place during the seeds producing. This is the worst thing for a specific variety seed grower. Therefore, a practical and efficient screening for foreign seeds or varieties would be very valuable.

Pepper (*Capsicum* spp.), belonging to the family of Solanaceae, is widely grown and used around the world as fresh vegetable and spice^[2]. Pepper includes essential nutrients for human metabolism such as polyphenols, carotenoids, capsaicinoids and ascorbic acid^[3-5]. In agricultural sector, variety discrimination of pepper seed is conducted by specialized technicians using traditional

Received date: 2015-03-09 **Accepted date:** 2015-12-22

Biographies: İlknur Alibas, PhD, Research Assistant, Research interests: Drying and precooling technologies of agricultural commodities, Email: ialibas@uludag.edu.tr; Ismail Kavdir, Professor, Research interests: NIR technologies, soft computing techniques in classification of agricultural commodities, Email: kavdiris@comu.edu.tr.

***Corresponding author:** Ferhat Kurtulmuş, PhD, Associate Professor, Research interests: Computer vision and machine learning applications in agriculture. Department of Biosystems Engineering, Faculty of Agriculture, Uludag University, 16059 Bursa, Turkey. Tel: +90-224-294-1600, Fax: +90-224-442-8775, E-mail: ferhatk@uludag.edu.tr.

methods. However, traditional methods are slow, hard to reproduce, and subjective^[6]. Besides, decision made by human experts may be different from person to person. Pepper varieties cannot be easily classified even by an expert eye due to the very small sizes of seeds and visual similarities. Hence, more advanced technologies are required to determine variety of pepper seeds rapidly and objectively. Computer vision and artificial intelligence methods could help determining the variety of pepper seeds in online industrial applications reducing processing time and labor significantly.

Various studies, involved in image processing and machine learning, were reported to determine the variety of seeds and grains primarily. An algorithm was proposed to distinguish kernels of wheat, barley, oats and rye based on color and shape features. They used Fourier transform to extract shape information. Classification was carried out by assigning different weights to the features. The shape was the most important attribute among the features used. In their study, classification accuracies of 100, 94, 93, 99, and 95% were accomplished^[7]. In another study, classification of weed seeds was studied at kernel level. They computed different type of features including morphological, color and texture. Neural network and naïve Bayes were used as classification models. With the proposed classification algorithms, classification scores varying between 90% and 100% were achieved^[6]. Corn kernels belonging to five varieties were classified based on image analysis: Mahalanobis distance discriminant and back propagation neural network were used as classifiers. Geometric, shape, and color features were calculated from corn kernels. Feature selection was performed with stepwise discriminant analysis. Mahalanobis distance and BPNN classifier were combined to constitute a classification model. Researchers reported that five corn varieties were classified with success rates over 90%^[8]. Nine wheat varieties were classified based on textural image features and linear discriminant analysis. A CCD (charge-coupled device) camera was used to acquire gray level of wheat images. Mass kernel imaging method was employed to capture the images of wheat varieties^[9]. With a stepwise discriminant analysis, 50 out of 131 total

texture features were selected according to their contribution to classification. Researchers reported that a classification accuracy of 98.15% was achieved for classifying nine wheat varieties. Another study, based on image analysis, focused on estimating phenolic maturity of grape seeds. Haralick texture descriptors were calculated as features after segmentation of grape seeds. Effective features were selected with sequential forward feature selection method. A multilayer perceptron was constructed to estimate phenolic maturity property of grape samples and a success rate of 100% was reported by Avila et al^[10]. Based on computer vision and principal component analysis, corn kernels were classified as damaged and healthy^[11]. Raw pixel values were used as features. Classification was carried out using a percentage ratio of defective area detected in the kernel image. Researchers could successfully determine damage status of corn kernels with a performance score of 90%. Barley varieties were classified using shape, color, and texture features^[12]. A flatbed scanner was used for image acquisition. In their study, barley samples were investigated at individual kernel level. Linear discriminant and principal component analyses were utilized to reduce the number of computed features. A three-layered neural network was performed to classify eleven barley varieties. Classification accuracies varying between 67% and 86% were reported. There is only one study involved in computer vision and pepper seed^[13]. Using basic seed features of color and size, they modeled a classification system to identify defective pepper seeds. They reported classification accuracies for abnormal seed color and unacceptable seed size as 95.82% and 90.76%, respectively.

Although several studies has been conducted involving computer vision and some seed varieties other than pepper, limited work has been reported on classification of pepper seed varieties including computer vision and neural networks. With this approach, the objective of this study was to develop a computer vision system based on neural networks and to determine the best feature model, and neural network topology yielding the best classification performance in recognizing pepper seed varieties from one another. Since simple, effective, and low cost image acquisition tools and techniques were

used, this study was unique.

2 Materials and methods

2.1 Seed samples

Eight varieties of *Capsicum* spp. were adopted in this research: Red sweet cherry, Red cheese pepper, Orozco hot pepper, Petit marseillais pepper, Chocolate habanero, Hot ancho grande, Red hot long thin cayenne, and Aci ilica.

The seeds were produced in Turkey in 2013, and obtained from a local seed producer. Before image acquisition, 832 undamaged seeds were selected manually to constitute a uniform representation of the varieties. Figure 1 is the scanned images of sample seeds used in this study.

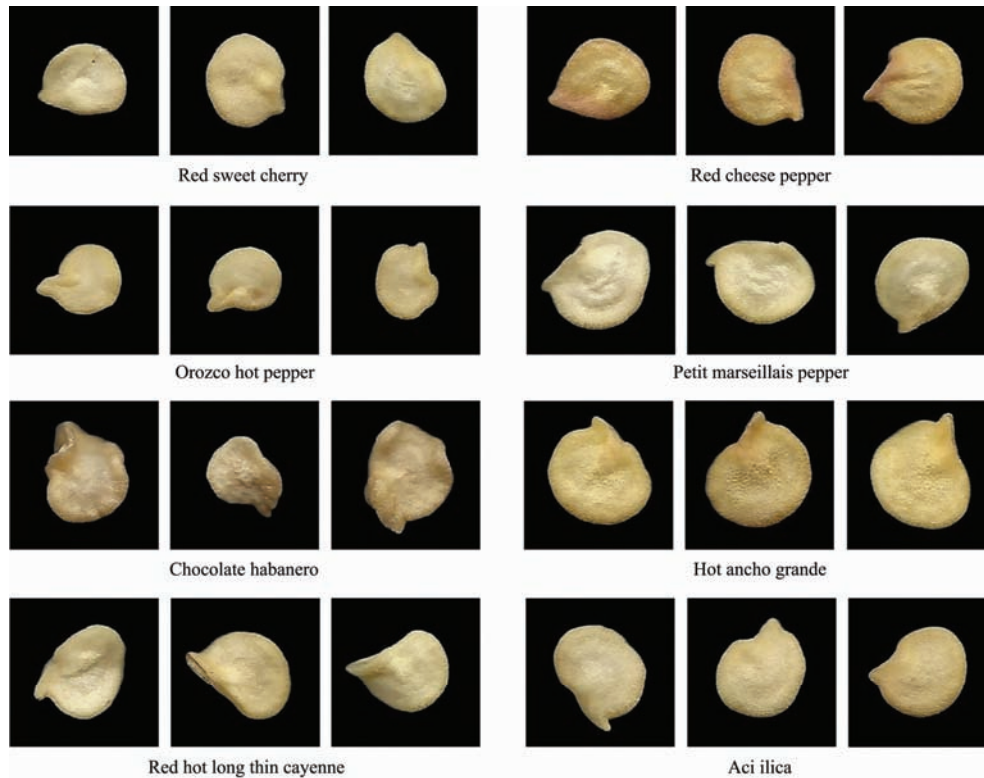


Figure 1 Sample seeds of eight varieties used in this study

2.2 Programming environment

In this research, Python 2.7 programming language was used for image processing steps such as seed segmentation and feature extraction with the help of Scipy and Numpy scientific computing libraries^[14]. Following programming libraries were utilized to implement image processing algorithms: Mahotas^[15], Scikit-image image processing library^[16], and OpenCV^[17]. Matlab (2012a, The MathWorks, Inc., Natick, Massachusetts) computing language was also used for implementing feature selection and neural networks.

2.3 Image acquisition

Image acquisition was conducted using an office scanner (Deskjet 1050A, Hewlett-Packard Comp., Palo Alto, California) at a resolution of 1200 dpi. Usage of a scanner has advantages such as it is less sensitive to illumination variations and it does not require additional

calibration processes (when it is turned on, it is automatically calibrated). A total of 104 pepper seeds for each variety were put on the scanner plate by preventing overlaps. Figure 2 shows the order of image processing tasks applied in this study.

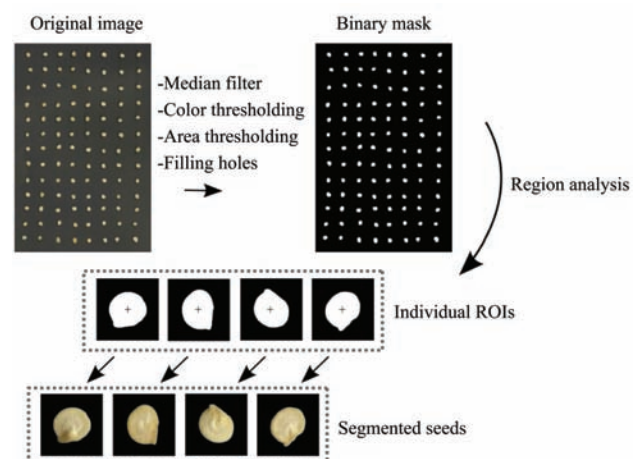


Figure 2 Image segmentation tasks applied to individual seed samples

Scanner plate was cleaned before each image acquisition process. A dark and low-reflective surface was placed on the pepper samples for an uniform imaging. Finally, a total of 832 (104×8) pepper seeds were scanned.

2.4 Segmentation of individual seed samples

In this research, each pepper seed was treated as an individual sample. Therefore, a segmentation process was needed to obtain region of interest (ROI) for each individual pepper seed. After image acquisition, non-touching pepper seeds were segmented using a sequence of image processing methods. For seed segmentation, the target was to obtain a proper mask for each sample as smooth as possible. Like other digitizer imaging devices, scanner also tries to interpolate boundary pixels between objects and backgrounds yielding mottled boundaries. However, this causes jagged edges of objects when segmentation is directly performed. To overcome this problem, a median filter was firstly applied to a scanned image to obtain smoother seed edges. The radius value of the median filter was determined as 8 to preserve characteristic shapes of the seeds and to obtain smoother edges. Since a dark background was used, a relatively simple thresholding method was enough to roughly obtain individual seed regions. With a trial-error method, it was found that red component and gray-level intensity map of the image were suitable for thresholding-based segmentation. The thresholding process used for binarization is described in Equation (1).

$$I_{mask} = \begin{cases} 1, & \text{If } I_{red} \geq \max(I_{red}) \times 0.33 \\ 0, & \text{If } I_{gray} < \max(I_{gray}) \times 0.34 \end{cases} \quad (1)$$

When images are scanned at a higher resolution (1200 dpi), even a smooth dark surface may have unwanted details considered as noise. Regions with the area value that was lower than a threshold (1000) were eliminated to remove unwanted noises. Once a binary mask was obtained, isolated small holes in the seed regions were filled with a morphological filling operation. A region analysis was applied to the binary mask for determining centroids of the seeds. Based on these centroids, 300×300 square ROI frames were superimposed on the original and unprocessed image to acquire individual seeds. As a result of masking

operation, background pixels in the RGB-colored ROI image were assigned as black, while keeping the original colors and textures of the seeds. Following this operation, individual seed images were stored to be used in further steps. Figure 2 summarizes the image segmentation processes applied in this study.

2.5 Feature extraction

Feature extraction process was applied on different color components of the images. RGB images were converted into two color spaces to be able to obtain different color components; namely, hue-saturation-intensity (HSI) and luminance-chrominance in blue-chrominance in red (YCbCr). Thus, features were extracted from eight color channels (R, G, B, H, S, I, Cb, and Cr). A total of 257 features were computed from segmented pepper seed images. Extracted features included basic color and shape features, Hu's invariant moments, Zernike moments, Haralick texture features, and circular Gabor texture features.

2.5.1 Basic color features

Basic color features for the images were obtained from 8 color components. Those features were mean (μ), standard deviation (σ), kurtosis (k), skewness (s), and mean Laplacian ($f''(x_{ij})$)^[18]. Equations of these features were provided in Appendix A. By computing these features for 8 color components, 40 basic color features were obtained.

2.5.2 Basic shape features

A total of 9 basic shape features were calculated in this study. Following basic shape features were calculated over the segmented binary images representing shape of the pepper seeds.

Area: number of pixels in pepper seed region of the binary image; convex area: number of pixels in the smallest convex polygon (convex hull) containing the pepper seed region; minor axis length: the length of the minor axis of the ellipse having the same normalized second central moments as pepper seed region; major axis length: the length of the major axis of the ellipse having the same normalized second central moments as pepper seed region; perimeter: perimeter of the region which approximates the contour as a line through the centers of border pixels of pepper seed; extent: ratio of pixels in

seed region to pixels in the total bounding box; solidity: the proportion of the pixels in the pepper seed region that are also in the convex hull; equivalent diameter: the diameter of a circle with the same area as the pepper seed region; roundness: roundness value of the pepper seed region computed using the ratio of perimeter $2/(4\pi \times \text{area})^{[16,18]}$.

2.5.3 Hu’s invariant moments

Hu’s invariant moments were used for shape recognition and identification process^[19]. Hu’s seven invariant moments were calculated over binary image, and they were invariant against affine transformations such as scale, translation and rotation^[20]. In this study, Hu’s seven invariant moments were calculated as given in Appendix A.

2.5.4 Zernike moments

Another kind of moments calculated in this research were Zernike moments. Zernike moments were calculated using a set of complex polynomials forming a complete orthogonal set over the interior of the unit circle ($x^2+y^2=1$)^[21,22]. In this research, Zernike moments up to the order 12 were calculated as suggested in the previous studies^[21-24]. Therefore, a total of 49 features were obtained to represent each segmented seed image.

2.5.5 Haralick texture features

Texture is distinctive information for recognizing objects in machine vision. A total of 14 texture features were suggested based on grey level co-occurrence matrix^[25]. In this research, these 14 texture features were also calculated for each pepper seed sample as described in literature [25] using Mahotas python module. By calculating these features for eight color components, 112 Haralick texture features were obtained. Features calculated were: maximal correlation coefficient, contrast, correlation, sum of squares, variance, inverse difference moment, sum average, sum variance, sum entropy, entropy, difference variance, difference entropy, information measure of correlation 1, information measure of correlation 2 and angular second moment.

2.5.6 Circular Gabor texture features

In this work, extraction of circular Gabor features was carried out according to the previous studies^[26,27]. For extracting texture information, individual pepper seed

images were convolved with circular Gabor function at five scales. A Gabor texture feature σ_G for any scale was calculated (Equation (2)) by taking standard deviation of resulting filtered-image I_g . This procedure was applied to eight color components. Thus, 40 circular Gabor texture features were obtained.

$$\sigma_G = \sqrt{\frac{1}{m \times n - 1} \sum_x \sum_y (|I_g(x, y) - \bar{I}_g|)^2} \quad (2)$$

2.6 Selection of effective features

2.6.1 Preparation data sets

It would be helpful to explain the formation of the data sets used in this study: first of all, the data was split into two subsets; development set (60%) and test set (40%). The test set was equally re-split into two parts called validation set (20%) and dedicated test set (20%) in the classification experiments. Development set was used for feature selection and training of the NN model while the dedicated test set was used only to examine the performance of a NN model. Eventually, three data sets were used as illustrated in Figure 3: development set, validation set, and dedicated test set.

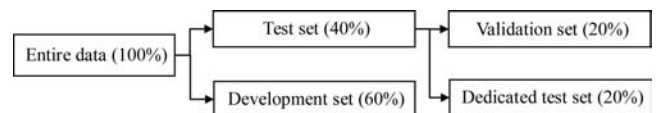


Figure 3 The formation of the data sets used in this study

2.6.2 Selection of effective features

Feature selection was used for reducing the dimensionality of the data by selecting a subset of calculated features, which was defined as the optimum feature model. Reducing features into an optimal subset provides many advantages such as avoiding overfitting, increasing model interpretability and lowering the computation time. In this research, forward sequential feature selection (SFS) method was employed for feature selection using ‘sequentialfs’ function of Matlab. Sequential feature selection starts with an empty feature set, and it sequentially includes a feature to create a candidate feature subset. Each candidate feature subset was evaluated by a criterion based on an error value from the classification performance of a cross-validated classifier. Four different machine learning classifiers were tried as the criterion function for the sequential feature selection; a discriminant analysis classifier, a

K-nearest-neighbor classifier, a naïve Bayes classifier, and a regression tree. Using development set of the data (training and validation), a 5-fold cross-validation process was performed for each criterion function yielding four different feature subsets (SFS_disc, SFS_knn, SFS_nB, and SFS_rt). In the cross-validation procedures, misclassification rate (MCE) was used as the criteria to minimize the error for the validation set.

2.7 Neural network setup

One of the most common neural network topologies is the multilayer perceptron (MLP). Its robustness has been proven in many classification tasks^[28-30]. A MLP is a feedforward artificial neural network consisting of a series of layers. Each neuron in the layers is connected to the neurons of the subsequent layer, and neurons sum up their inputs passing the results through activation functions^[31]. Figure 4 shows the MLP topology used in this work. As can be seen in previous studies, a single hidden layer containing sufficient number of neurons can satisfactorily perform the prediction of most complex problems^[32,33]. In this research, a hidden layered MLP topology was chosen, and implemented using the 'patternnet' function in Matlab (2012a, The MathWorks, Inc., Natick, Massachusetts). This function uses hyperbolic tangent sigmoid transfer function (Equation (3)) to compute a layer's output from its input. Therefore, hyperbolic tangent sigmoid transfer functions were used in the hidden and output layers of the MLP NN.

$$\text{Tansig}(n) = \frac{2}{1 + e^{-2n}} - 1 \quad (3)$$

Three different training algorithms were performed to minimize training error in this research: scaled conjugate gradient (trainscg), resilient back propagation (trainrp), and variable learning rate back propagation (traingdx)^[34,35]. Performances of these algorithms were evaluated separately.

The scaled conjugate gradient algorithm (trainscg) combines the gradient descent with the Levenberg–Marquardt algorithm, and it is designed for large-scale problems^[12,36]. In this algorithm, the length of weight updating period is depended on the learning rate. The search orientation and the duration of weight updating are selected via the second-order approximation of the error function^[35,36].

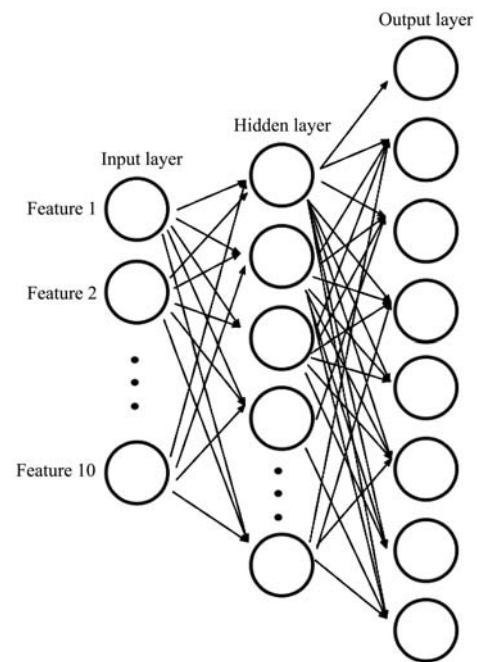


Figure 4 The MLP topology used in the study

The resilient back propagation (trainrp)^[37] is another modification of the standard back propagation. This algorithm eliminates unfavorable influence of the magnitudes of the partial derivatives in back propagation method. It performs the weight adaptation process according to the sign of the derivative^[38,39]. More detailed information about this algorithm can be found in reference [37].

Gradient descent with a variable learning rate and momentum (traingdx) is a training algorithm which updates weight and bias values using gradient descent momentum and an adaptive learning rate. To calculate the derivatives of performance, back propagation was utilized according to the weight and bias variables. Learning rate is increased during training iterations if the performance decreases^[34].

Another important parameter of MLP topology is the number of neurons in the hidden layer. Although there are some rules of thumb methods for determining the number of neurons in the hidden layer, most of these techniques are empirical^[40,41]. It is always reasonable to try a wide range of neurons to determine the best topology. In this research, different MLP architectures were created and tested using neuron numbers from 5 to 70 with the increment value of 5. To avoid overfitting, the training (60% of the data) and validation sets (20% of the data) were used to tune the weights during the training

iterations. After training stage, the MLP model was tested using a test set (20% of the data) consisting of samples totally unseen by the model. All the steps were repeated for each of the four different feature subsets to seek the superior model in classifying pepper seed samples.

3 Results and discussion

3.1 Optimum feature set

Purpose of this study was to determine the best MLP topology and an optimum feature set for the classification of pepper seed images using color, shape, and texture features. A sequential feature selection was performed on the development set of the data with four different criterion functions to determine an optimum feature set.

As a result of cross-validated sequential feature selection, four different feature sets were obtained as given in Table 1. Each feature set was a combination of the features representing color, shape, and texture, meaning that at least one of these feature types had a contribution to discriminating the variety of a pepper seed. As also inferred from Table 1, different color components were effective for classifying pepper seeds. Moreover, feature sets primarily included features belonging to R, G, and B components. In this research, the number of features was significantly reduced from 257 to a range between 10 and 12 to help avoiding overfitting. Also, decrease in the number of features helps the implementation of classification algorithms lower the processing times significantly in real world applications.

Table 1 Four feature sets obtained from sequential feature selection using different criterion functions.

	SFS_disc	SFS_knn	SFS_nB	SFS_rt
1	Mean[G]	Mean[G]	Std[R]	Mean[B]
2	Mean Laplace[R]	Kurtosis[G]	Std[G]	Mean Laplace[B]
3	Hu moments 2(Φ_2)	Kurtosis[Cr]	Entropy[V]	Angular Second Moment[V]
4	Solidity	Skewness[B]	Maximal Correlation Coefficient[V]	Sum of Squares: Variance[V]
5	Entropy[R]	Hu Moments 1(Φ_1)	Correlation[G]	Information Measure of Correlation 2[G]
6	Sum of Squares: Variance[B]	Solidity	Difference Variance[B]	Difference Variance[B]
7	Inverse Difference Moment[B]	Difference Entropy[R]	Maximal Correlation Coefficient[S]	Sum Average[H]
8	Information Measure of Correlation 1[B]	Information Measure of Correlation 2[G]	Circular Gabor(G, 4)	Difference Entropy[H]
9	Circular Gabor[B, 5]	Difference Variance[B]	Circular Gabor(H, 5)	Information Measure of Correlation 2[S]
10	zernike_moments[9]	Information Measure of Correlation 2[S]	Zernike moments[22]	Circular Gabor[V, 5]
11		Zernike Moments[36]	Zernike moments[37]	Zernike Moments[40]
12			Zernike moments[38]	Zernike Moments[45]

Note: Each entry in the table represents a feature. Letters in square brackets represent color channel. Numbers in square brackets after comma represent queue number of any feature vector.

3.2 The best network topology

The MLP models were trained with the data including different features from feature selection methods. Percentage accuracies of different MLP models using the test data are shown in Table 2. In this research, several MLP models performed accuracy rates higher than 80% in classification experiments. Considering all the feature models, mean accuracy rates for trainrp, trainscg, and trainidx were 76.32%, 66.19%, and 67.56%, respectively. Based on the mean accuracy values obtained from the training algorithms used in this study, trainrp outperformed the others in pepper seed classification.

As inferred from Table 2, most of the MLP models accomplished classification of 8 pepper seeds with accuracy rates over 70%. Moreover, for each feature set, at least three MLP models achieved classification of pepper seeds with accuracy rates over 80% using 40 and higher number of neurons in the hidden layer. On the other hand, classification scores over 80% could also be obtained using the neuron numbers lower than 35 with the feature set of SFS_disc and the training algorithm of resilient back propagation. This result was important because it is always better to obtain a high performance with a low number of neurons in the hidden layer with MLPs. It should also be noted here that the feature set

of SFS_disc had the lowest number of features (10) among the feature sets used. Thus, it can be concluded that the best classification performances were obtained using the feature set of SFS_disc. And, the best

classification accuracy was found to be 84.94% with the feature set of SFS_disc, the training algorithm of resilient back propagation, and 30 neurons in the hidden layer.

Table 2 Percentage accuracies of different MLP models on the test data

N. of neurons in the hidden layer	Feature set											
	SFS_disc (10 features)			SFS_knn (11 features)			SFS_nB (12 features)			SFS_rt (12 features)		
	Training algorithm			Training algorithm			Training algorithm			Training algorithm		
	trainrp	trainscg	traingdx	trainrp	trainscg	traingdx	trainrp	trainscg	traingdx	trainrp	trainscg	traingdx
5	73.49%	41.57%	69.88%	75.90%	66.87%	11.45%	67.47%	70.48%	16.27%	70.48%	54.82%	16.27%
10	78.92%	26.51%	65.66%	69.28%	59.64%	25.90%	78.31%	50.60%	74.10%	77.11%	54.82%	69.88%
15	77.11%	79.52%	60.24%	77.71%	81.93%	72.29%	77.11%	75.90%	74.10%	74.70%	77.71%	74.70%
20	77.71%	46.99%	71.08%	74.10%	54.22%	61.45%	73.49%	27.11%	78.92%	75.90%	72.89%	74.10%
25	81.33%	44.58%	78.92%	77.71%	71.69%	65.66%	76.51%	69.88%	77.11%	71.69%	75.90%	75.90%
30	84.94%	81.93%	79.52%	72.89%	54.22%	72.29%	78.92%	47.59%	76.51%	77.11%	75.90%	75.30%
35	77.71%	77.71%	21.08%	74.10%	74.70%	74.70%	75.30%	60.84%	20.48%	79.52%	74.70%	81.33%
40	81.33%	48.19%	69.28%	81.33%	80.72%	78.92%	78.31%	81.33%	82.53%	81.93%	80.12%	80.72%
45	80.72%	56.63%	71.08%	78.31%	77.71%	77.71%	74.10%	77.71%	76.51%	73.49%	60.84%	71.08%
50	79.52%	65.66%	75.30%	78.31%	76.51%	74.70%	76.51%	72.29%	68.67%	72.89%	44.58%	66.87%
55	75.90%	77.71%	74.10%	73.49%	41.57%	71.08%	77.71%	78.31%	71.08%	75.30%	74.10%	71.69%
60	77.71%	77.71%	72.29%	77.71%	80.12%	72.29%	79.52%	78.31%	77.11%	76.51%	43.37%	76.51%
65	82.53%	80.72%	73.49%	71.69%	77.71%	74.70%	74.10%	80.12%	78.92%	75.90%	75.90%	74.70%
70	72.89%	73.49%	69.28%	72.89%	47.59%	70.48%	74.70%	75.30%	77.11%	72.29%	71.08%	69.88%

3.3 Training record

It was crucial to make sure if any overfitting had happened even though the classification results were cross validated. Training record is a good indicator for detecting these types of problems. In Figure 5, training record of the best-scored MLP model was given illustrating mean squares errors at each iteration performed for training, validation and testing. Validation and test curves were quite similar in Figure 5.

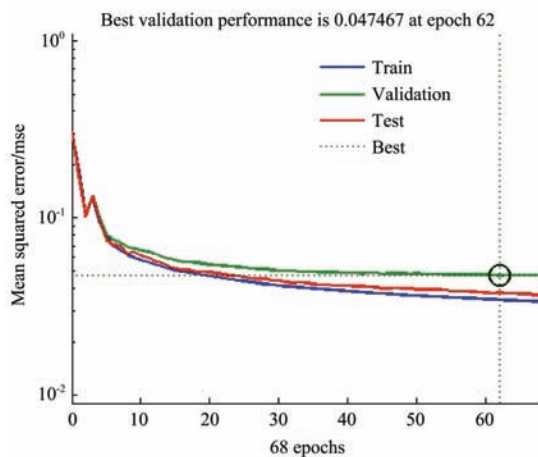


Figure 5 MSE curves during training stage

Also, there was not any increase in the test error before the validation error increased. Therefore, it can

be concluded that there was no overfitting in training stage of the best MLP model, and the model is reliable in this manner.

3.4 Classification accuracy

Detailed performance results were given only for the best MLP model as it would take too much space to do it for all the MLP results tested. A total of 166 test samples (20% of the data) were evaluated. Detailed performance results for the best MLP model are given in Figure 6. The confusion matrix in Figure 6 illustrates the misclassifications between the pepper varieties. While diagonal entries of the confusion matrix were correct classifications, the rest of non-zero matrix entries represented misclassifications. The last row and the last column show the measures of recall (or sensitivity) and precision, respectively illustrating classification performances at class level. Major misclassifications occurred in discriminating between Red hot long thin cayenne versus Aci ilica and between Red sweet cherry versus Petit marseillais pepper (4 misclassifications for each couple). The MLP model failed especially in discriminating Aci ilica and Petit marseillais peppers resulting low classification accuracies. The highest

recall rate was obtained for Orozco hot pepper seeds meaning that Orozco hot pepper was the most distinctive variety investigated in this research in term of image features. A total of 24 samples belonging to this variety were classified correctly by the MLP model. However, two samples belonging to other varieties were misclassified as Orozco hot pepper.

classification accuracies varying between 67% and 86% were reported for identifying barley varieties, which were similar to the results obtained in this study. This study was the first effort to classify pepper seed varieties using neural network and computer vision. Considering close similarities among the pepper seed varieties, the accuracy rates obtained from the classification experiments conducted in this study can be assumed promising, although further work is needed to constitute an online sorting system with more precise classification algorithm. As an overall result obtained from this research, scanner images and MLP method can be used as a technique for discrimination of pepper seed varieties based on image features. Since the MLP models were constructed by considering overfitting and cross validation rules, the method proposed in this study offers a reliable and unbiased solution for discriminating pepper seeds. The technique which was proposed in this study has a good potential to be used among seed producers. It will enable seed producers to perform successful screening of their products to avoid foreign seeds or varieties get involved in their packages.

Confusion Matrix

Output Class	Aci ilica	21 12.7%	0 0.0%	0 0.0%	0 0.0%	1 0.6%	0 0.0%	0 0.0%	1 0.6%	91.3%	8.7%
	Chocolate habanero	2 1.2%	19 11.4%	0 0.0%	0 0.0%	0 0.0%	0 0.0%	0 0.0%	0 0.0%	90.5%	9.5%
	Hot ancho grande	0 0.0%	0 0.0%	19 11.4%	0 0.0%	0 0.0%	0 0.0%	0 0.0%	0 0.0%	100%	0.0%
	Orozco hot pepper	0 0.0%	1 0.6%	0 0.0%	24 14.5%	0 0.0%	0 0.0%	0 0.0%	1 0.6%	92.3%	7.7%
	Petit marseillais pepper	1 0.6%	0 0.0%	0 0.0%	0 0.0%	10 6.0%	1 0.6%	0 0.0%	1 0.6%	76.9%	23.1%
	Red cheese pepper	0 0.0%	0 0.0%	2 1.2%	0 0.0%	2 1.2%	18 10.8%	0 0.0%	0 0.0%	81.8%	18.2%
	Red sweet cherry	0 0.0%	0 0.0%	0 0.0%	0 0.0%	4 2.4%	1 0.6%	12 7.2%	2 1.2%	63.2%	36.8%
	Red hot long thin cayenne	4 2.4%	0 0.0%	0 0.0%	0 0.0%	0 0.0%	0 0.0%	1 0.6%	18 10.8%	78.3%	21.7%
			75.0%	95.0%	90.5%	100%	58.8%	90.0%	92.3%	78.3%	84.9%
		25.0%	5.0%	9.5%	0.0%	41.2%	10.0%	7.7%	21.7%	15.1%	
		Aci ilica	Chocolate habanero	Hot ancho grande	Orozco hot pepper	Petit marseillais pepper	Red cheese pepper	Red sweet cherry	Red hot long thin cayenne		
		Target Class									

Figure 6 Confusion matrix of the MLP model with the best setting

Low numbers of the features including shape, color, and texture used in this work were enough to construct a MLP model for classification of pepper seeds. The best classification accuracy was achieved using only 10 features avoiding overfitting. Considering feature set of SFS_disc (Table 1), which resulted in the best classification performance, 4 features out of 10 were texture-based implying that texture plays an important role discriminating the variety of pepper seeds. In this study, which features were more effective on pepper seed classification and which MLP topology was superior with individual seed images were shown. These results also provided good contributions to the literature reported on the classification of seeds. In this research, the best performance in pepper seed classification was as high as the results obtained in most of the previously reported studies which worked on classification of some other grain and seed varieties^[9,13]. However in literature [13],

4 Conclusions

- 1) A classification method was proposed to discriminate pepper seeds based on MLP and computer vision. By calculating features from different color components, a large feature database was constructed and relevant features were selected using sequential feature selection with different criterion functions. A 5-fold cross-validation process was utilized for each criterion function yielding four different feature sets. A large range for the number of neurons in the hidden layer was investigated to determine the best MLP model. In addition, three types of training algorithms were studied.
- 2) Kernel imaging method with a regular scanner can be an affordable inspection tool to determine variety of pepper seed.
- 3) With the computer vision system developed, accuracy rates over 80% (84.94% for the best MLP topology) were obtained in classifying eight pepper seed varieties by avoiding overfitting.
- 4) Sequential feature selection method with

discriminant analysis can increase accuracy of pepper seed classification.

5) Usage of the resilient back propagation algorithm improves classification accuracy.

Although the classification accuracy achieved in this study has not been high enough to constitute a ready-to-use classification system, the results obtained are promising. One limitation of the presented work was the necessity of manually setting pepper seeds for their non-touching arrangement in the scanner tray. On the other hand, this study has focused on determining the best MLP topology and feature set for pepper seed classification. Further studies are required to increase the classification accuracy by using various machine learning classifiers and features, especially should include an advanced segmentation algorithm to cope with randomly occluded pepper seeds. Proposed system should also be enhanced to incorporate additional pepper and other seed varieties in addition to the existing variety database.

Appendix A

Basic color features:

Following equations were used for calculating basic color features^[18,42].

Mean:

$$\mu = \frac{1}{n} \sum_{i=1}^n x_{ij} \quad (A1)$$

Standard deviation:

$$\sigma = \sqrt{\frac{1}{n} \sum_{i=1}^n (x_{ij} - \bar{x})^2} \quad (A2)$$

Kurtosis:

$$k = \frac{\frac{1}{n} \sum_{i=1}^n (x_{ij} - \bar{x})^4}{\left(\frac{1}{n} \sum_{i=1}^n (x_{ij} - \bar{x})^2\right)^2} \quad (A3)$$

Skewness:

$$S = \frac{\frac{1}{n} \sum_{i=1}^n (x_{ij} - \bar{x})^3}{\left(\frac{1}{n} \sum_{i=1}^n (x_{ij} - \bar{x})^2\right)^{3/2}} \quad (A4)$$

Mean Laplacian:

$$f''(x_{ij}) = \frac{f'(x_{ij}) - f'(x_{ij-1})}{(ij+1) - ij} \quad (A5)$$

where, n is the number of pixels, and x_{ij} denotes the pixel value of any color component.

Hu's invariant moments:

For a two dimensional function $f(m,n)$, geometric moment of order $(p + q)$ of an image was defined in Equation (A6)^[22].

$$M_{pq} = \sum_{m=1}^M \sum_{n=1}^N m^p n^q f(m,n) \quad (A6)$$

Using the components of the centroid (x_c, y_c) , the previous definition was rewritten in Equation (A7) to obtain central moments. Hu's 7 invariant moments were computed by normalizing the central moments as defined in Equations (A9-A15)^[22,23].

$$\mu_{pq} = \sum_{m=1}^M \sum_{n=1}^N (m - x_c)^p (n - y_c)^q f(m,n); \quad (A7)$$

$$x_c = \frac{M_{10}}{M_{00}}, \quad y_c = \frac{M_{01}}{M_{00}}$$

$$\eta_{pq} = \frac{\mu_{pq}}{\mu_{00}^\gamma}; \quad \gamma = (p + q) / 2 \quad (A8)$$

$$\Phi_1 = \eta_{20} + \eta_{02} \quad (A9)$$

$$\Phi_2 = (\eta_{20} - \eta_{02})^2 + 4\eta_{11}^2 \quad (A10)$$

$$\Phi_3 = (\eta_{30} - 3\eta_{12})^2 + (\eta_{03} - 3\eta_{21})^2 \quad (A11)$$

$$\Phi_4 = (\eta_{30} + \eta_{12})^2 + (\eta_{03} + \eta_{21})^2 \quad (A12)$$

$$\Phi_5 = (3\eta_{30} - 3\eta_{12})(\eta_{30} + \eta_{12})[(\eta_{30} + \eta_{12})^2 - 3(\eta_{03} + \eta_{21})^2] + (3\eta_{21} - \eta_{03})(\eta_{03} + \eta_{21}) \cdot [3(\eta_{30} + \eta_{12})^2 - (\eta_{03} + \eta_{21})^2] \quad (A13)$$

$$\Phi_6 = (\eta_{20} - \eta_{02})[(\eta_{30} + \eta_{12})^2 - (\eta_{21} - \eta_{03})^2] + 4\eta_{11}(\eta_{30} + \eta_{12})(\eta_{21} + \eta_{03}) \quad (A14)$$

$$\Phi_7 = (3\eta_{21} - \eta_{03})(\eta_{30} + \eta_{12})[(\eta_{30} + \eta_{12})^2 - 3(\eta_{03} + \eta_{21})^2] + (3\eta_{12} - \eta_{30})(\eta_{21} + \eta_{03}) \cdot [3(\eta_{30} + \eta_{12})^2 - (\eta_{21} + \eta_{03})^2] \quad (A15)$$

[References]

- [1] Chen X, Xun Y, Li W, Zhang J. Combining discriminant analysis and neural networks for corn variety identification. *Computers and Electronics in Agriculture*, 2010; 71: S48-S53.
- [2] Bae H, Jayaprakasha G K, Jifon J, Patil B S. Variation of antioxidant activity and the levels of bioactive compounds in lipophilic and hydrophilic extracts from hot pepper (*Capsicum spp.*) cultivars. *Food Chemistry*, 2012; 134: 1912-1918.

- [3] Alvarez-Parrilla E, de la Rosa L A, Amarowicz R, Shahidi F. Antioxidant activity of fresh and processed Jalapeño and serrano peppers. *Journal of Agricultural and Food Chemistry*, 2010; 59: 163–173.
- [4] Hervert-Hernández D, Sáyago-Ayerdi S G, Goñi I. Bioactive compounds of four hot pepper varieties (*Capsicum annuum* L.), antioxidant capacity, and intestinal bioaccessibility. *Journal of Agricultural and Food Chemistry*, 2010; 58: 3399–3406.
- [5] Jeong W Y, Jin J S, Cho Y A, Lee J H, Park S, Jeong S W, et al. Determination of polyphenols in three *Capsicum annuum* L. (bell pepper) varieties using high-performance liquid chromatography–tandem mass spectrometry: Their contribution to overall antioxidant and anticancer activity. *Journal of Separation Science*, 2011; 34: 2967–2974.
- [6] Granitto P M, Navone H D, Verdes P F, Ceccatto H A. Weed seeds identification by machine vision. *Computers and Electronics in Agriculture*, 2002; 33: 91–103.
- [7] Paliwal J, Shashidhar N S, Jayas D S. Grain kernel identification using kernel signature. *Transactions of the ASAE*, 1999; 42: 1921–1924.
- [8] Chen X, Xun Y, Li W, Zhang J. Combining discriminant analysis and neural networks for corn variety identification. *Computers and Electronics in Agriculture*, 2010; 71(1): S48–S53.
- [9] Pourreza A, Pourreza H, Abbaspour-Fard M H, Sadrnia H. Identification of nine Iranian wheat seed varieties by textural analysis with image processing. *Computers and Electronics in Agriculture*, 2012; 83: 102–108.
- [10] Avila F, Mora M, Fredes C. A method to estimate Grape Phenolic Maturity based on seed images. *Computers and Electronics in Agriculture*, 2014; 101, 76–83.
- [11] Valiente-Gonzalez J M, Andreu-Garcia G, Potter P, Rodas-Jorda A. Automatic corn (*Zea mays*) kernel inspection system using novelty detection based on principal component analysis. *Biosystems Engineering*, 2014; 117: 94–103.
- [12] Szczypiński P M, Klepaczko A, Zapotoczny P. Identifying barley varieties by computer vision. *Computers and Electronics in Agriculture*, 2015; 110, 1–8.
- [13] Chupawa P, Kanjanawanishkul K. Sweet Pepper Seed Inspection Using Image Processing Techniques. *Advanced Materials Research*, 2014; 931-932: 1614–1618.
- [14] Oliphant T E. Python for scientific computing. *Computing in Science and Engineering*, 2007; 9(3), 10–20.
- [15] Coelho L P. Mahotas: Open source software for scriptable computer vision. *Journal of Open Research Software*, 2013; 1(1): e3. doi: <http://dx.doi.org/10.5334/jors.ac>.
- [16] Walt S V D, Schönberger J L, Nunez-Iglesias J, Boulogne F, Warner J D, Yager N, et al. Scikit-image: Image processing in Python. *Peer J*, 2014; 2:e453.
- [17] OpenCV. Open source computer vision. Available at: www.opencv.org. Accessed October 4, 2014.
- [18] Donis-González I R, Guyer D E, Leiva-Valenzuela G A, Burns J. Assessment of chestnut (*Castanea* spp.) slice quality using color images. *Journal of Food Engineering*, 2013; 115: 407–414.
- [19] Hu M K. Visual pattern recognition by moment invariants. *IRE Transactions on Information Theory*, 1962; 8(2): 179–187.
- [20] Chen Q, Petriu E, Yang X. A comparative study of Fourier descriptors and Hu's seven moment invariants for image recognition. *Electrical and Computer Engineering, Canadian Conference on*, 2004; p103-106.
- [21] Teague M. Image analysis via the general theory of moments. *Journal of the Optical Society of America*, 1980; 70(8): 920–930.
- [22] Wang J, He J, Han Y, Ouyang C, Li D. An adaptive thresholding algorithm of field leaf image. *Computers and Electronics in Agriculture*, 2013; 96: 23–39.
- [23] Ding M Y, Chang J L, Peng J X. Research on moment invariant algorithm. *Journal of Data Acquisition and Processing*, 1992; 7(1): 1–9.
- [24] Wang X F, Huang D S, Du J X, Xu H, Heutte L. Classification of plant leaf images with complicated background. *Applied Mathematics and Computation*, 2008; 205(2): 916–926.
- [25] Haralick R M. Statistical and structural approaches to texture. *Proc. IEEE*, 1979; 67(5): 786–804.
- [26] Zhang J, Tan T, Ma L. Invariant texture segmentation via circular Gabor filters. *16th International Conference on Pattern Recognition (ICPR 2002)*, 11-15 August 2002, Quebec, Canada.
- [27] Kurtulmuş F, Lee W S, Vardar A. Green citrus detection using 'eigenfruit', color and circular Gabor texture features under natural outdoor conditions. *Computers and Electronics in Agriculture*, 2011; 78(2): 140–149.
- [28] Aghbashlo M, Mobli H, Rafiee S, Madadlou M. The use of artificial neural network to predict exergetic performance of spray drying process: A preliminary study. *Computers and Electronics in Agriculture*, 2012; 88: 32-43.
- [29] Boniecki P, Koszela K, Piekarska-Boniecka H, Weres J, Zaborowicz M, Kujawa S, et al. Neural identification of selected apple pests. *Computers and Electronics in Agriculture*, 2015; 110: 9–16.
- [30] Kujawa S, Nowakowski K, Tomczak R J, Dach J, Boniecki P, Weres J, et al. Neural image analysis for maturity classification of sewage sludge composted with maize straw. *Computers and Electronics in Agriculture*, 2014; 109:

- 302–310.
- [31] Omid M, Mahmoudi A, Omid M H. An intelligent system for sorting pistachio nut varieties. *Expert Systems with Applications*, 2009; 36(9): 11528–11535.
- [32] Nazghelichi T, Aghbashlo M, Kianmehra M H. Optimization of an artificial neural network topology using coupled response surface methodology and genetic algorithm for fluidized bed drying. *Computers and Electronics in Agriculture*, 2011; 75(1): 84–91.
- [33] Wang W, Paliwal J. Generalisation performance of artificial neural networks for near infrared spectral analysis. *Biosystems Engineering*, 2006; 94(1): 7–18.
- [34] Beale M H, Hagan M T, Demuth H B. *Neural Network Toolbox User's Guide*. The MathWorks, Inc., 2014; Natick, MA, USA.
- [35] Craninx M, Fievez V, Vlaeminck B, De Baets B. Artificial neural network models of the rumen fermentation pattern in dairy cattle. *Computers and Electronics in Agriculture*, 2008; 60(2): 226–238.
- [36] Møller M F. A scaled conjugate gradient algorithm for fast supervised learning. *Neural Networks*, 1993; 6(4): 525–533.
- [37] Riedmiller M, Braun H. A direct adaptive method for faster backpropagation learning: the RPROP algorithm. *Proceedings of the IEEE International Conference on Neural Networks*, 1993; 1, p586–591.
- [38] Patnaik L M, Rajan K. Target detection through image processing and resilient propagation algorithms. *Neurocomputing*, 2000; 35(1–4): 123–135.
- [39] Santra A K, Chakraborty N, Sen S. Prediction of heat transfer due to presence of copper–water nanofluid using resilient-propagation neural network. *International Journal of Thermal Sciences*, 2009; 48(7): 1311–1318.
- [40] Heaton J. *Introduction to Neural Networks for Java: Feedforward Backpropagation Neural Networks*. Available at: <http://www.heatonresearch.com/node/707>. Accessed on [2014-10-04].
- [41] Priddy K L, Keller P E. *Artificial Neural Networks: An Introduction (SPIE Tutorial Texts in Optical Engineering, Vol. TT68)*, The International Society for Optical Engineering, 2005; Bellingham, Washington, USA.
- [42] Nixon M S, Aguado A S. *Feature Extraction and Image Processing*. Elsevier, 2008; London, UK.